Stability and Dissociation Dynamics of the Low-Lying Excited States of Ozone

M. C. Garner, K. A. Hanold, M. Sowa Resat, and R. E. Continetti*

Department of Chemistry and Biochemistry, 0314, University of California, San Diego, 9500 Gilman Drive, La Jolla, California 92093-0314

Received: January 28, 1997; In Final Form: March 27, 1997[⊗]

This paper reports an investigation of the stability and dissociation dynamics of the low-lying singlet and triplet states of ozone (O_3) using coincident photoelectron and photofragment translational spectroscopy. These experiments provide an upper limit of 0.5 μs for the lifetime of the low-lying excited states of O_3. The $^3A_2$ and $^3B_2$ states dissociate with nearly all available energy appearing in translation. Dissociation of the higher-lying $^3B_1$ and $^1A_2$ states produces rotationally and possibly vibrationally excited O_2 products. The product translational energy distributions indicate that the $^3B_1$ state dissociates nonadiabatically to ground-state $O(^3P) + O_2(^3\Sigma_g^-)$ products.

1. Introduction

The recognition of ozone (O_3) depletion in the stratosphere[1] has resulted in an intense focus on the mechanisms of atmospheric O_3 formation and destruction.[2] An important question concerns the possible existence of bound excited states of O_3. Kinetic studies have suggested that a bound low-lying excited state may explain discrepancies observed in measured rates of ozone production through the important three-body recombination reaction $O + O_2 + M \rightarrow O_3 + M$.[3] A metastable singlet state of D_{3h} symmetry has been predicted to exist[4−7] and may play a role in this reaction. This species has yet to be observed. There are, however, three known low-lying triplet states ($^3A_2$, $^3B_2$, and $^3B_1$) of O_3 which are poorly characterized. Recent experimental studies have indicated that these states all lie above the energy required for dissociation of O_3 into ground-state $O + O_2$ products.[8−10] There have been no direct measurements of either the stability or dissociation dynamics of these states. We have undertaken such measurements using coincident photoelectron and photofragment translational spectroscopy.

Absorption and emission spectroscopy have been used to study the well-known Hartley, Huggins, Chappuis, and Wulf bands of O_3.[2] These features extend from approximately 200−1100 nm and are generally diffuse with some vibronic structure. The $^1A_1$ ground state of O_3 and spin-selection rules led to the initial assignment of these bands to transitions involving the singlet excited states. Optical excitation of the triplet excited states from the singlet ground state is spin-forbidden and is expected to occur with only a small absorption cross section. These optical selection rules dictate that the numerous recent studies of the dissociation dynamics of O_3 have been restricted to the singlet excited states.[11]

Recent theoretical and experimental studies have suggested that the low-lying triplet states may explain vibronic structure in the Wulf band.[12−16] High-sensitivity absorption spectroscopy[8,9,14] has been used to study these very weak transitions. Recent work by Bouvier et al.[9] has provided high-resolution absorption spectra from 8600 to 10 500 cm^{-1}. These spectra reveal rotational structure superimposed on the origin and first bending vibration transitions, assigned to the $^3A_2$ electronic state.[9] An estimated radiative lifetime of 0.01−0.1 s for this state was obtained from the Einstein coefficients and Franck−Condon factors with the ground state of O_3.[9] This is an upper limit to the actual lifetime. Pressure and Doppler broadening in these experiments prevented measurement of reliable homogeneous line widths < 0.07 cm^{-1}, corresponding to a lower limit of the lifetime ≈ 0.1 ns.

Optically forbidden excited states can also be studied using electron spectroscopies, since the optical spin-selection rules do not apply in such experiments. Swanson and Celotta were the first to use electron-energy-loss spectroscopy in a study of the low-lying triplet states.[17] A number of more recent studies of electron energy loss[18] and dissociative electron attachment[19,20] experiments have significantly extended our knowledge of both anionic and neutral excited states of ozone. The electron affinity of O_3 has been determined by both photodetachment cross section measurements[21] and photoelectron spectroscopy of O_3^-.[22] Recently, Arnold et al.[10] reported high-resolution photoelectron spectra that reveal features assigned to the five lowest excited states of O_3. The energetics determined in these recent experiments are in good agreement with absorption spectroscopy.[8] In particular, it is evident that the three low-lying triplet states lie above the lowest $O(^3P) + O_2(^3\Sigma_g^-)$ dissociation asymptote.

There have also been numerous theoretical studies of the ground and excited states of O_3.[6,7,12,13,16,24,25] The ordering and energies of the excited states vary considerably with the level of theory applied. In some of the larger ab initio studies Banichevich et al.[23] and Braunstein et al.[13] have discovered conical intersections among low-lying states in C_s symmetry. Recent multiconfigurational perturbation theory calculations by Tsuneda et al.[24] and Borowski et al.[25] have supported the photoelectron assignments of Arnold et al.[10] except for the $^3B_1$ and $^3B_2$ states which the calculations show to be nearly degenerate. Although some of the earlier calculations indicated that one or more of the low-lying triplet states may be bound with respect to dissociation,[23,26] the most recent calculations predict no bound excited states.[24,25]

The experiments described here directly address the question of the stability and dissociation dynamics of the low-lying electronic states of O_3. The low-lying excited states which are spin- and/or dipole-forbidden with respect to the ground state of O_3 are prepared by fully allowed one-electron photodetachment transitions from the $^2B_1$ ground state of O_3^-. In the next section, the technique of coincident photoelectron and translational spectroscopy is described. In section 3 the results including photoelectron spectra and correlation spectra of the

* Corresponding author. E-mail: rcontinetti@ucsd.edu. Tel: (619)-534-5559 FAX: (619)-534-7042.

[⊗] Abstract published in *Advance ACS Abstracts,* July 15, 1997.

S1089-5639(97)00351-4 CCC: $14.00

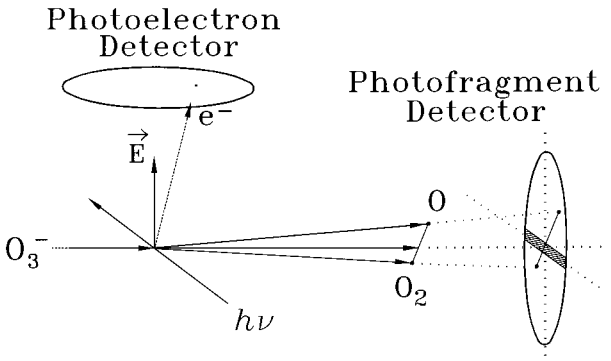

Figure 1. Schematic view of the detection geometry. A fast ion beam is intersected at a right angle by a photodetachment laser. Recoil velocities and angles of the photoelectron and photofragments are measured. The "vertical" laser polarization is shown (electric vector **E** perpendicular to the ion beam direction). The hatched region on the photofragment detector shows the beam-block.

photoelectron kinetic energy and the photofragment translational energy release are presented. Finally, in section 4, a discussion of the implications of these data on the stability and dissociation dynamics of these states is given.

2. Experimental Section

These experiments make use of coincident photoelectron and photofragment translational spectroscopy in a fast ion beam. The low-lying excited states of O_3 are prepared by photodetachment of O_3^- at 266 nm. The measured photoelectron energy determines which state of O_3 is produced. The subsequent dissociation dynamics of O_3 are studied by translational energy spectroscopy of the $O + O_2$ photofragments. This combination of spectroscopies provides a unique measurement of the partitioning of energy, on an event-by-event basis, in the dissociative photodetachment of O_3^-. The spectrometer used in these experiments has been described previously[27] and will be only briefly reviewed here.

A schematic view of the apparatus detection geometry is shown in Figure 1. O_3^- is generated by electron impact on a mixture of $O_2 + O_3$ in a pulsed free-jet expansion. The anions are accelerated (beam energies range from 2 to 6 keV) and mass selected by time-of-flight. The O_3^- is then intersected by the linearly polarized fourth harmonic (266 nm, 4.66 eV) of a pulsed Nd:YAG laser.[28] Spectra are recorded with the laser polarization vector, **E**, either perpendicular ("vertical", as shown in Figure 1) or parallel ("horizontal") to the ion beam direction.

The photoelectron spectrometer employs a time- and position-sensitive electron detector to measure the laboratory kinetic energy by time-of-flight and electron recoil angle by detected position. Measurement of the electron recoil angle is essential to allow correction for the Doppler broadening due to the fast ion beam.[27] With this correction, the electron kinetic energy in the center-of-mass frame (eKE) is determined. The photoelectron spectra can be recorded in coincidence with stable O_3 or $O + O_2$ photofragments.

Translational energy spectroscopy is performed by recording the time- and position-of-arrival of coincident O and O_2. Residual ions and any ionic photofragments are removed from the beam by electrostatic deflection. At 266 nm, photodetachment is the dominant photodestruction mechanism. Neutral photofragments recoil out of the beam over a 96 cm flight path between the laser interaction region and the photofragment detector. The photofragments that clear a 7 mm wide beam-block impinge on a time- and position-sensitive detector. The angular acceptance of the photofragment detector is ≈25% of 4π sr given the kinematics of $O + O_2$ dissociation.

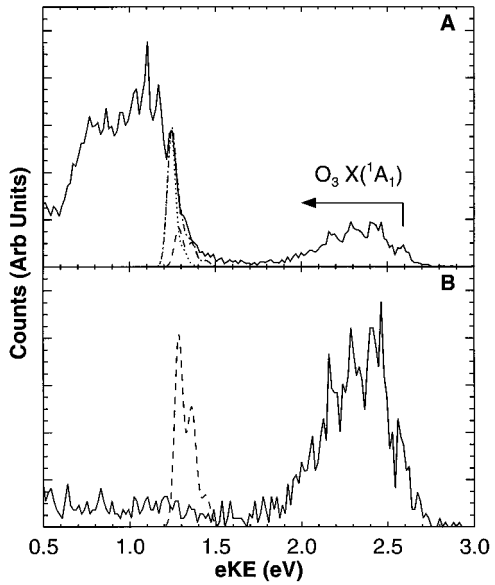

Figure 2. Photoelectron kinetic energy spectra with the photofragment detector beam-block removed for the horizontal laser polarization. Frame A includes contributions from both stable and dissociating O_3. Frame B includes contributions from only stable O_3 and false coincidences. Dashed lines are Franck−Condon fits; see text for details.

Correlation of the photoelectron with the photofragments is ensured by carrying out the experiment such that ≈0.1 dissociation event occurs per laser shot, giving <10% false coincidences for three particles. Conservation of linear momentum between each $O-O_2$ photofragment pair is checked to ensure that they originate in a single dissociative event. Photofragment mass, center-of-mass translational energy release (E_T), recoil angle, and eKE are then calculated for each event. The translational energy resolution of the apparatus is ≤10% $\Delta E/E$ (fwhm) and the eKE resolution is ≈4% $\Delta E/E$ (fwhm).[27]

3. Results

3.1. Photoelectron Spectra. The simplest measurement involved looking for stable O_3 in coincidence with photoelectrons from photodetachment to the excited states of O_3. In this measurement the beam block was removed so undissociated O_3 could be detected. In Figure 2A the eKE spectrum for the horizontal polarization is shown. Photoelectron spectra recorded under these conditions show a feature in the range 1.7 eV < eKE < 3.0 eV corresponding to production of ground-state O_3 ($\tilde{X}\ ^1A_1$). Also shown is a Franck−Condon simulation of the $^3A_2$ ($\nu_2' = 0-1$) and $^3B_2$ ($\nu_2' = 0$) excited-state region of the spectrum, eKE ≈ 1.1−1.5 eV. This simulation, adapted from the results of Arnold et al.,[10] assumes a 450 K vibrational temperature of the anion to account for the hot bands evident at ≈1.4 eV. The simulation is seen to fit the leading edge of the excited-state photoelectron signal and can be used as an indication of the expected signature of stable excited states. The photoelectron spectrum of the *stable* states of O_3 is shown in Figure 2B. Stable O_3 is identified by the arrival at the photofragment detector of a single particle at the beam velocity in coincidence with a photoelectron. Also shown in this frame is the Franck−Condon fit from Frame A for the $^3A_2$ ($\nu_2' =$ 0,1) states which have been suggested to be long-lived by Bouvier et al.[9] No evidence of stable O_3 is observed in the $^3A_2$ region other than false coincidence background. Thus, while O_3 ($\tilde{X}\ ^1A_1$) is stable, the excited states dissociate faster than the 6 μs flight time to the detector at a beam energy of 6 keV. A further test involved comparisons of the photofragment translational energy release spectra at beam energies of 2.5 and

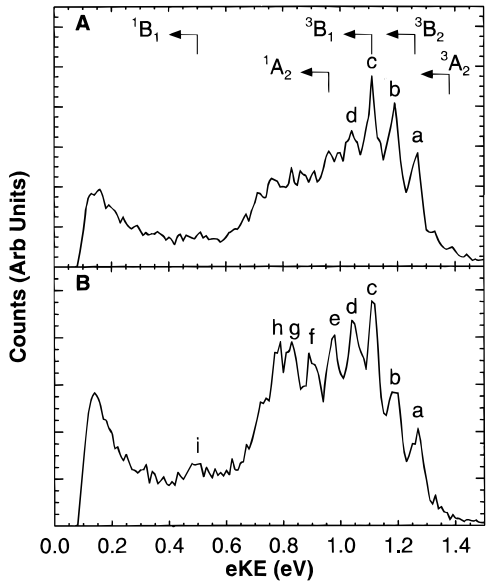

Figure 3. Photoelectron kinetic energy spectra of the dissociative states of O_3 at 266 nm at a beam energy of 2.5 keV. Frames A and B show horizontal and vertical polarization data, respectively. Assignments for the five low-lying states $^3A_2$, $^3B_2$, $^3B_1$, $^1A_2$, and $^1B_1$ of Arnold et al.[10] are shown. See Table 1 for the energies of the labeled peaks.

TABLE 1: Peak Positions in eKE and E_T for the Labeled Features in Figures 3 and 4[a]

feature	eKE (eV)	E_T (eV)	fwhm (eV)	E_{ROT} (eV)
a	1.27	0.23	0.08	0.01
b	1.19	0.29	0.09	0.03
c	1.12	0.36	0.15	0.03
d	1.05	0.39	0.21	0.07
e	0.98	0.41	0.25	0.12
f	0.90	0.43	0.30	0.18
g	0.83	0.43	0.30	0.25
h	0.78	0.43	0.30	0.30

[a] These values were taken from the vertical polarization data in Figure 4B. The values are consistent with the horizontal data to ±0.01 eV. The fwhm (full width at half-maximum) for E_T slices at the specified eKE are also shown. The estimated rotational energies, E_{ROT}, are determined by the difference of the total kinetic energy at the peak of each feature from the maximum translational energy for [$O(^3P)$ + $O_2(^3\Sigma_g^-,v=0)$ + e^-] products. E_{ROT} assumes no vibrational excitation of the O_2 fragment and has an estimated error of ±0.03 eV.

4.0 keV. If the excited states have a lifetime greater than 0.5 μs, the apparent E_T would be reduced at the higher beam energy. These measurements indicated that the excited states dissociate promptly.

Photoelectron spectra recorded from the dissociative states of O_3 are shown in Figure 3. The top and bottom frames of Figure 3 show data recorded with horizontal and vertical laser polarizations, respectively. The differences in these spectra result from anisotropic photoelectron angular distributions for the dissociative states of O_3. The spectra in Figure 3 are consistent with the high-resolution photoelectron study of Arnold et al.[10] The horizontal polarization eKE spectrum (Figure 3A) shows several prominent peaks labeled (a−d). The peak positions of these and other features are summarized in Table 1. These peaks, spaced by 70−80 meV, were assigned by Arnold et al.[10] to overlapping bending vibrations in the three lowest triplet states, $^3A_2$, $^3B_2$, and $^3B_1$. The vertical polarization spectrum (Figure 3B) shows further resolved structure in the 0.5−1.0 eV range (peaks e−i). The structure from 0.6 to 1.0 eV was assigned to overlapping transitions to the $^3B_1$ and $^1A_2$ states, while feature i at 0.5 eV was assigned to the $^1B_1$ state of O_3.[10] All eKE spectra show a peak at low energy (0.12 eV)

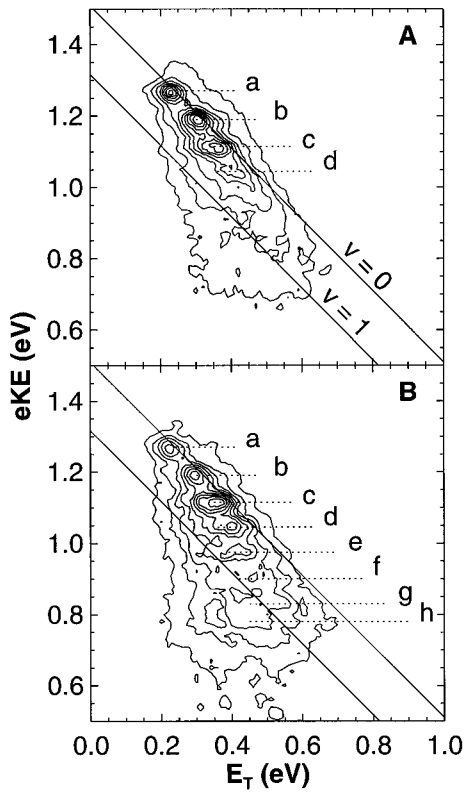

Figure 4. $N(E_T,eKE)$ correlation spectrum of the electron kinetic energy (eKE) and the translational energy release (E_T) between the O + O_2 photofragments. Energetic thresholds for [$O(^3P)$ + $O_2(^3\Sigma_g^-,v=0)$ + e^-] and [$O(^3P)$ + $O_2(^3\Sigma_g^-,v=1)$ + e^-] are also shown. Frames A and B show horizontal and vertical polarization data, respectively. The labeled features correspond to the peaks in the contour map *and* the photoelectron spectra in Figure 3. The photoelectron kinetic energy axis is truncated at 0.5 eV as no significant features are observed in the correlation spectrum below that energy. Ten evenly spaced contours represent the number of counts in each two dimensional bin, smoothed by a boxcar average over three 0.01 × 0.01 eV wide bins.

which results from stray laser-induced photoelectrons. This background signal peaks at low energy and falls off rapidly with little contribution to the spectra beyond 0.5 eV.

3.2. Correlation Spectra. These experiments measure the correlation between the photoelectron kinetic energy and the photofragment center-of-mass translational energy release. The observation of resolved structure in the photoelectron spectra indicates that the dissociative states of O_3 survive for more than a vibrational period (≈10^{-14} s). Thus, this coincidence measurement allows one to study the predissociation dynamics of internal-energy-selected O_3 excited states. In these measurements it is also possible to examine angular correlations between the photoelectron and photofragment recoil directions.[27] No evidence for such correlations was found in these measurements, confirming that photodetachment and subsequent dissociation of the excited states occurs on a time-scale much greater than a rotational period (≈10^{-11} s).

Figure 4 shows the results from the coincidence measurement as a correlation spectrum of eKE and E_T, $N(E_T,eKE)$. These spectra are two-dimensional histograms accumulated from approximately 40 000 events each. Spectra for horizontal and vertical laser polarizations are shown in Figure 4A,B, respectively. The two diagonal lines represent the maximum translational energy limits for the production of ground-state photofragments [$O(^3P)$ + $O_2(^3\Sigma_g^-,v=0)$ + e^-] and photofragments with one quantum of vibration in O_2 [$O(^3P)$ + $O_2(^3\Sigma_g^-,v=1)$ + e^-]. These thresholds are determined from the photon energy ($E_{h\nu}$= 4.66 eV at 266 nm), the electron

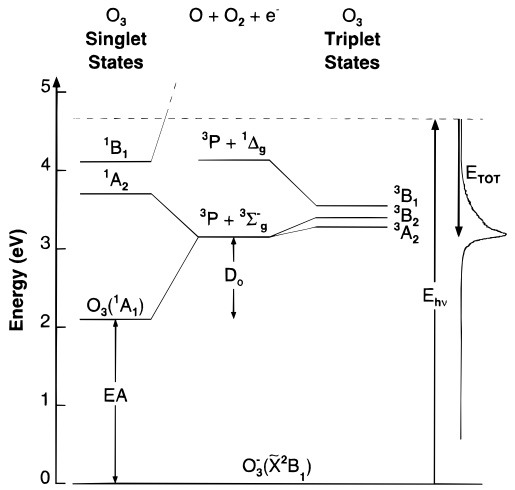

Figure 5. Energetics diagram for O_3^- and O_3, showing the total translational energy release spectrum (E_{TOT} = eKE + E_T). The electronic states are labeled in C_{2v} symmetry, and the energetics are defined in the text. The adiabatic correlations between states and photoproducts are also shown. The ordering of the excited states is from Arnold et al.[10]

affinity of O_3 (EA = 2.103 eV),[22] the O−O_2 bond dissociation energy (D_0 = 1.05 eV),[29] and the $O_2(^3\Sigma_g^-)$ vibrational quantum (ΔE = 0.193 eV).[30] The estimated uncertainty in the $N(E_T$,eKE) peak positions is ±0.03 eV. The contours extend over the maximum translational energy limit for $\nu = 0$, indicating the production of some internally excited O_3^- in the ion source.[31]

There are four prominent peaks evident in the contours of the correlation spectra (Figure 4). In the horizontal polarization (Figure 4A) the three peaks (a−c, see Table 1) are arrayed along the translational energy limit corresponding to ground-state products. Thus, nearly all the available energy is appearing in translation with very little vibrational or rotational energy for these dissociation events. In the vertical polarization (Figure 4B) there are four peaks (a−d). In addition, bands are observed that correspond to the peaks (e−h) in the photoelectron spectra. This shows that photofragments produced in coincidence with lower electron kinetic energies ($^3B_1$ and $^1A_2$ states) yield products with a broader distribution of rotational and/or vibrational excitation. The peaks and widths of the E_T distributions at the center of each photoelectron peak are given in Table 1. In addition, an estimate of the rotational energy in O_2 for these peaks is determined by the difference of the total kinetic energy for these features from the maximum translational energy threshold (see Table 1). This estimate ignores the possible contributions of vibrational excitation to the width in E_T of features (f−h).

An energy level diagram for O_3^- and O_3 is shown in Figure 5. This diagram uses the energetics of Arnold et al.[10] and shows the adiabatic correlations between the excited states and the dissociation channels.[6] In addition, the total translational energy release spectrum (E_{TOT} = eKE + E_T) is shown vertically on the right side of Figure 5. The E_{TOT} spectrum shows that dissociative photodetachment of O_3^- yields only ground electronic state products [$O(^3P) + O_2(^3\Sigma_g^-) + e^-$]. The $^1A_2$, $^3A_2$, and $^3B_2$ states adiabatically correlate with the observed ground-state products. The $^3B_1$ state, however, correlates to [$O(^3P) + O_2(^1\Delta_g)$] and is well below this dissociation asymptote. Dissociation of the $^3B_1$ state to ground-state products must occur by a nonadiabatic interaction.

4. Discussion

4.1. Excited-State Lifetimes. The results presented here show that the low-lying excited states of O_3 dissociate promptly, with an upper limit to the dissociation lifetime of 0.5 μs. An important question concerns how these measurements compare to the recent work of Bouvier et al.[9] Rovibronic fine-structure observed in their experiment indicates the presence of a barrier to dissociation of the two lowest bending vibrations of the $^3A_2$ state.[8,9] The small difference in equilibrium bond angles between the ground-state neutral (116.6°) and the anion (115.5°)[24] indicates that photodetachment and optical excitation should access similar Franck−Condon regions in the bending coordinate of the excited states. The Franck−Condon region in the symmetric stretch is quite different, however, due to the fact that the O−O bond length of the ground-state anion (1.376 Å) is similar to the calculated value of the $^3A_2$ state (1.369 Å), while the ground-state neutral has a much shorter bond length of 1.291 Å.[24] Therefore the photoelectron spectra are dominated by bending excitation, while optical absorption should produce both bend and stretch excitation. The O_3^- produced by electron impact in a pulsed supersonic jet is expected to have rotational temperatures on the order of 50 K,[32] so it is anticipated that photodetachment will primarily produce low rotational levels in the $^3A_2$ state. Thus, it is expected that photodetachment of O_3^- should effectively populate the $^3A_2$ levels observed by Bouvier et al.[9] In conjunction with the line widths observed by Bouvier et al., our results indicate a range of 0.1−500 ns for the lifetime of the $\nu_2 = 0,1$ levels of the $^3A_2$ state.

4.2. Dissociation Dynamics. The $N(E_T$,eKE) correlation spectra show that dissociation of the two lowest triplet states ($^3A_2$ and $^3B_2$) leads to virtually all the available energy appearing in translation. For the $^3B_1$ and $^1A_2$ states, considerably more energy appears in rotation and/or vibration of the O_2 product. The results also indicate that the $^3B_1$ state dissociates nonadiabatically to ground electronic state products.

Dissociation of the low-lying excited states of O_3 is likely to proceed by distortion from C_{2v} to C_s symmetry along the asymmetric stretch coordinate. An alternative mechanism, involving elimination of the central O atom and preserving C_{2v} symmetry may also be considered.[22] Elimination of the central O atom would be expected to produce significant vibrational excitation of the nascent O_2 fragment. The asymmetric dissociation mechanism, on the other hand, is expected to yield a large fraction of energy in translation along with some rotational and vibrational excitation, which is more consistent with the observed dynamics. In the low levels of the $^3A_2$ and $^3B_2$ states there is no evidence at all of vibrational excitation. As dissociation of the $^3B_1$ and $^1A_2$ states occurs, more energy appears in rotation and perhaps vibration as well. The absence of resolved O_2 vibrational states in the translational energy distribution indicates, however, that rotational excitation in excess of the vibrational spacing of O_2 occurs in this energy range. These results are most consistent with the asymmetric dissociation pathway.

Levene and Valentini have discussed the photodissociation dynamics of O_3 in the Huggins band in terms of a modified impulse model, in which the partitioning of energy between translation and rotation is determined by the impulse along the breaking bond.[33] In this model, impulsive vibrational excitation is ignored and the product vibrational distribution was found to be approximated by a Franck−Condon distribution between the excited state of O_3 and the product O_2. These dynamics may provide a qualitative explanation of the product translational energy distribution for dissociation of the $^1A_2$ and $^3B_1$ states (peaks d−h in the $N(E_T$,eKE) correlation spectra).

The modified impulse model apparently fails to describe dissociation of the low levels of the $^3A_2$ and $^3B_2$ states. Peaks a−c in Figure 4, assigned to these states, exhibit no product vibrational and little rotational excitation. This model predicts 0.06 eV in rotation for peak a if one uses the equilibrium bond angle of the $^3A_2$ state of 99.2°.[24] This is significantly larger than the nominal observed value of 0.01 eV. The impulse model can, of course, still work if it is arbitrarily assumed that the excited molecule distorts into a more linear configuration before the bond breaks impulsively. A factor that may contribute to the breakdown of the impulse approximation is the small available energy in dissociation of the $^3A_2$ and $^3B_2$ states. The small repulsion between the products provides greater opportunity for exit channel interactions, contrary to the fundamental assumption of a sudden impulse. As Schinke has pointed out, the details of the bending potential and exit channel interactions can play a crucial role in rotational excitation.[34] As more detailed potential energy surfaces for the low-lying states of O_3 become available, it should be possible to carry out realistic dynamics calculations to compare with the present experiments.

4.3. Nonadiabatic Dissociation of the $^3B_1$ State. The nonadiabatic dissociation of the $^3B_1$ state further confirms that the excited-state dynamics of O_3 are complicated and is also consistent with the asymmetric dissociation pathway. Theoretical studies have shown that there are both singlet and triplet conical intersections in C_s symmetry involving the $^1B_1$, $^1A_2$ and $^3B_1$, $^3A_2$ states, respectively.[12,24] Thus, it is most likely that dissociation of the $^3B_1$ state to ground-state products occurs through this interaction with the lower $^3A_2$ state. The singlet-state conical intersection has been previously invoked by Braunstein et al.[12] to explain the observation by Levene et al.[33] of only ground-state products [$O(^3P) + O_2(^3\Sigma_g^-)$] after excitation to the $^1B_1$ state. In that case, the $^1B_1$ state is known to adiabatically correlate to higher energy $O(^1D) + O_2(^1\Delta_g)$ products. In a similar fashion, dissociation of the $^3B_1$ state to ground-state products can occur after a crossing to the $^3A_2$ surface.

In C_{2v} symmetry the $^3A_2$ and $^3B_1$ states cross, however, they become the two lowest $^3A''$ states in C_s symmetry, forming the conical intersection.[12] As dissociation begins along the asymmetric stretch coordinate, the molecular symmetry drops to C_s and the molecule may find itself on the lower dissociative surface. Tsuneda et al.[24] have determined that the conical intersection between the $^3A_2$ and $^3B_1$ states should lie near the $^3A_2$ equilibrium geometry.[24] O_3^- ($\tilde{X}\ ^2B_1$) has a bond angle of 115.5° while the $^3A_2$ and $^3B_1$ states of O_3 have bond angles of 99.2° and 123.7°, respectively.[24] The large difference in bond angles between O_3^- and the O_3 $^3B_1$ state is expected to yield significant bending excitation upon photodetachment. This bending excitation may promote sampling of the conical intersection leading to facile dissociation of the $^3B_1$ state to ground-state photoproducts via the intermediate $^3A_2$ state. It is interesting to note that peak c in the correlation spectra, assigned to the $^3B_1$ state by Arnold et al.,[10] marks the beginning of the trend to greater rotational excitation in the O_2 products. This may be a direct signature of the nonadiabatic interaction and should provide an important test of future theoretical models of this dissociation.

5. Conclusion

In conclusion, we report direct measurements of the stability and dissociation dynamics of the low-lying triplet states of ozone. The data presented here show that the triplet states of ozone have lifetimes of $<0.5\ \mu$s. The correlation between the electron kinetic energy and the photofragment translational energy reveals features that show dissociation of the low-lying triplet states ($^3A_2$, $^3B_2$, and/or $^3B_1$) primarily produce little or no vibrational excitation in the O_2 photofragment. Rotational excitation of the O_2 products is also lower than predicted by simple impulse models of rotational excitation for these bent states. The observation of ground-state products from the $^3B_1$ state indicates that the dissociation dynamics are complicated by nonadiabatic interactions and merit further study.

The short lifetimes of the low-lying excited states of O_3 indicate that bimolecular chemistry of the triplet states will not be an important chemical process in the atmosphere. In addition, the short lifetime of the triplet states shows that these states cannot be responsible for discrepancies in kinetic studies of the O_3 recombination reaction. If significant long-lived excited states of O_3 exist, they must originate from unobserved species such as cyclic-O_3 that have poor Franck−Condon overlap with the ground states of O_3 or O_3^-.

Acknowledgment. This work was supported by the Chemistry Division of the National Science Foundation (CHE-9321786). R.E.C. is a David and Lucile Packard Fellow in Science and Engineering and a Camille Dreyfus Teacher-Scholar. We thank an anonymous reviewer for some interesting comments.

References and Notes

(1) Rowland, F. S.; Molina, M. J. *Rev. Geophys. Space Phys.* **1975**, *13*, 1. Reid, G. C.; McAfee, J. R.; Crutzen, P. J. *Nature* **1978**, *275*, 489.
(2) See the review article: Steinfeld, J. I.; Adler-Golden, S. M.; Gallagher, J. W. *J. Phys. Chem. Ref. Data* **1987**, *16*, 911.
(3) Locker, J. R.; Joens, J. A.; Blair, E. J. *J. Photochem.* **1987**, *36*, 235.
(4) Lee, T. J. *Chem. Phys. Lett.* **1990**, *169*, 529.
(5) Xantheas, S. S.; Atchity, G. J.; Elbert, S. T.; Ruedenberg, K. *J. Chem. Phys.* **1991**, *94*, 805.
(6) Hay P. J.; Dunning, Jr., T. H. *J. Chem. Phys.* **1977**, *67*, 2290.
(7) Banichevich, A.; Peyerimhoff, S. D. *Chem. Phys.* **1993**, *174*, 93.
(8) Anderson, S. M.; Mauersberger, K. *J. Geophys. Res.* **1995**, *100*, 3033.
(9) Bouvier, A. J.; Bacis, R.; Bussery, B.; Churassy, S.; Inard, D.; Nota, M.; Brion, J.; Malicet, J.; Anderson, S. M. *Chem. Phys. Lett.* **1996**, *255*, 263.
(10) Arnold, D. W.; Xu, C.; Kim E. H.; Neumark, D. M. *J. Chem. Phys.* **1994**, *101*, 912.
(11) Levene, H. B.; Nieh, J.-C.; Valentini, J. J. *J. Chem. Phys.* **1987**, *87*, 2583. Kinugawa, T.; Sato, T.; Arikawa, T.; Matsumi, Y.; Kawasaki, M. *J. Chem. Phys.* **1990**, *93*, 3289. Daniels, M.; Wiesenfeld, J. R. *J. Chem. Phys.* **1993**, *98*, 321. Suits, A. G.; Miller, R. L.; Bontuyan, L. S.; Houston, P. L. *J. Chem. Soc., Faraday Trans.* **1993**, *89*, 1443. Thelen, M.-A.; Gejo, T.; Harrison, J. A.; Huber, J. R. *J. Chem. Phys.* **1995**, *103*, 7946. Stranges, D.; Yang, X.; Chesko, J. D.; Suits, A. G. *J. Chem. Phys.* **1995**, *102*, 6067.
(12) Braunstein, M.; Hay, P. J.; Martin, R. L.; Pack, R. T. *J. Chem. Phys.* **1991**, *95*, 8239.
(13) Braunstein M.; Pack, R. T. *J. Chem. Phys.* **1992**, *96*, 6378.
(14) Anderson, S. M.; Hupalo, P.; Mauersberger, K. *J. Chem. Phys.* **1993**, *99*, 737.
(15) Minaev B.; Ågren, H. *Chem. Phys. Lett.* **1994**, *217*, 531.
(16) Braunstein, M.; Martin, R. L.; Hay, P. J. *J. Chem. Phys.* **1995**, *102*, 3662.
(17) Swanson, N.; Celotta, R. J. *Phys. Rev. Lett.* **1975**, *35*, 783.
(18) Allan, M.; Mason N. J.; Davies, J. A. *J. Chem. Phys.* **1996**, *105*, 5665. Mason, N. J.; Gingell, J. M.; Davies, J. A.; Zhao, H.; Walker, I. C.; Siggel, M. R. F. *J. Phys. B* **1996**, *29*, 3075.
(19) Allan, M.; Asmis, K. R.; Popovic, D. B.; Stepanovic, M.; Mason, N. J.; Davies, J. A. *J. Phys. B* **1996**, *29*, 4727. Walker, I. C.; Gingell, J. M.; Mason, N. J.; Marston, G. *J. Phys. B* **1996**, *29*, 4749.
(20) Skalny, J. D.; Matejcik, S.; Kiendler, A.; Stamatovic, A.; Märk, T. D. *Chem. Phys. Lett.* **1996**, *255*, 112.
(21) Wang, L. J.; Woo, S. B.; Helmy, E. M. *Phys. Rev. A* **1987**, *35*, 759.
(22) Novick, S. E.; Engelking, P. A.; Jones, P. L.; Futrell, J. H.; Lineberger, W. C. *J. Chem. Phys.* **1979**, *70*, 2652.
(23) Banichevich, A.; Peyerimhoff, S. D. *Chem. Phys.* **1993**, *178*, 155.

(24) Tsuneda, T.; Nakano, H.; Hirao, K. *J. Chem. Phys.* **1995**, *103*, 6520.

(25) Borowski, P.; Fulscher, M.; Malmqvist, P.; Roos, B. O. *Chem. Phys. Lett.* **1995**, *237*, 195.

(26) Wilson, C. W.; Hopper, D. G. *J. Chem. Phys.* **1981**, *74*, 595.

(27) Hanold, K. A.; Sherwood, C. R.; Garner, M. C.; Continetti, R. E. *Rev. Sci. Instrum.* **1995**, *66*, 5507. Hanold, K. A.; Garner, M. C.; Continetti, R. E. *Phys. Rev. Lett.* **1996**, *77*, 3335.

(28) Xie, X.; Simon, J. D. *Opt. Commun.* **1989**, *69*, 303.

(29) Gole, J. L.; Zare, R. N. *J. Chem. Phys.* **1972**, *57*, 5331.

(30) Huber, K. P.; Herzberg, G. *Molecular Spectra and Molecular Structure IV. Constants of Diatomic Molecules*; Van Nostrand: New York, 1979; pp 491−499.

(31) Garner, M. C.; Sherwood, C. R.; Hanold, K. A.; Continetti, R. E. *Chem. Phys. Lett*. **1996**, *248*, 20.

(32) Continetti, R. E.; Cyr, D. R.; Metz, R. B.; Neumark, D. M. *Chem. Phys. Lett.* **1991,** *182*, 406.

(33) Levene, H. B.; Valentini, J. J. *J. Chem. Phys.* **1987**, *87*, 2594.

(34) Schinke, R. *Photodissociation Dynamics*; Cambridge Press: Cambridge, UK, 1993; pp 251−255.